BULLETIN *of the*
MALAYSIAN MATHEMATICAL
SCIENCES SOCIETY
http://math.usm.my/bulletin

Bull. Malays. Math. Sci. Soc. (2) **36***(1) (2013), 7–22*

On Vorticity Prediction Using Limited Rotated Richtmyer Scheme

FARZAD ISMAIL
School of Aerospace Engineering, Universiti Sains Malaysia, 14300 Pulau Pinang, Malaysia
aefarzad@eng.usm.my

Abstract. In this paper, a study on limited Rotated Richtmyer scheme is performed with a focus on vorticity prediction. It will be mathematically and numerically demonstrated that the Rotated Richtmyer scheme coupled with a TVD limiter can retain both irrotational and rotational flow when solving pure acoustics equations. However, the limited Rotated Richtmyer scheme cannot preserve irrotational flow if the advection terms are included.

2010 Mathematics Subject Classification: 76N15, 35L05, 35Q31

Keywords and phrases: Vorticity prediction, finite volume method, TVD limiter, linearized Euler.

1. Introduction

In aerospace engineering, the problem of shock wave and vortex interaction (SVI) occurs in many compressible flow applications. SVI is present in aircraft or missile travelling at supersonic (or hypersonic) speeds where the shock interacts with the vortices shed by the body and in air-fuel mixing environment inside a supersonic ramjet engine [14]. In helicopter analysis, SVI occurs when the helicopter blades rotate at transonic speeds creating a shockwave which interact with the trailing vortices shed by the blades themselves [12]. This is also known as the blade-vortex-interaction (BVI) problem. Overall, it is very difficult to accurately predict vortical flows since most numerical schemes will excessively dissipate or spuriously create vorticity [10], and it is even more challenging to predict vortical flows interacting with a shockwave [5]. Perhaps in SVI problems where either the shock or vortex are relatively weak, reasonably accurate predictions can be obtained using the currently available schemes [13] but this not the case when both shock and vortex are strong. In fact, for strong SVI problems there are cases such that negative pressure, temperature and density are reported using the current state-of-the-art numerical schemes [14].

In the current state-of-the-art numerical schemes, the science of conserving (or preserving) primary variables such mass, momentum and energy is a mature field [15]. However, there is still more to be explored when attempting to conserve secondary variables. In terms of entropy conservation (or production) which is a very important feature in aerodynamics,

Communicated by Ahmad Izani Md. Ismail.
Received: August 24, 2011; *Revised:* February 3, 2012.

there exists the work of [19], and more recently [9]. The work of [17] deals with conservation of total kinetic energy which is relevant to turbulent flows. The work of [13] and [16] discuss entropy-consistent schemes for computing complex turbulent flows. In terms of preserving vorticity as a secondary variable, the underlying challenge lies in discretely solving a nonlinear system of equations with discrete differential constraints.

Morton and Roe [11] developed an elegant method of exactly preserving discrete vorticity based on the second order accurate Rotated Richtmyer scheme. The notion of vorticity preserving scheme is based on that the numerical errors produced will not create vorticity. Similar methods have also been developed [3, 10]. However, none of these schemes address the use of limiters. The use of limiters is essential to circumvent Godunov's theorem [4] in predicting data with large gradients such as shocks using second order accurate methods (or higher) without generating spurious oscillations.

Ismail and Roe [8] were the first to develop limited Godunov-type vorticity preserving schemes, providing an avenue for conventional finite volume schemes coupled with the classic TVD/TVB limiters [6]. However, the method requires subiterations within each time step to ensure that the predicted vorticity is consistent with an independent vorticity transport estimate thus adding computational cost. These subiterations are analogous to preserving the $\nabla \cdot \vec{u} = 0$ in incompressible flow. The limited Rotated Richtmyer scheme will be more economical if it remains vorticity preserving. Of course, an alternative path in producing accurate vortical flow predictions is to use very high order accurate schemes such as WENO [13] since the generation of vorticity errors are directly proportional to the magnitude of local truncation errors of the scheme [11]. However, these high order schemes are usually less robust in complex computations and are more sensitive to the deterioration of the order of accuracy under grid distortions [7] hence less suited for practical CFD.

The objective of this paper is to analyze a limited [6] Rotated Richtmyer (RR) scheme [11] when predicting vorticity in the system of linearized Euler equations. Although vorticity is naturally a 3D phenomena, but for start only simple 2D vortical flows are studied here. Note that the focus of this paper will be strictly on inviscid fluid although there have been viscous-vortex studies [2, 1]. Section 2 will present the vorticity preserving scheme developed by [11]. In Section 3, some mathematical analyses will be done to show that the limited version of this scheme strictly cannot preserve vorticity when solving the linearized isothermal Euler equations. Numerical results will be provided in Section 4. Finally, Section 5 will draw a conclusion to the paper.

2. Vorticity analysis in 2D acoustic equations

The work of Morton and Roe [11] will be now revisited. Define 2D vorticity $\tilde{\omega} = v_x - u_y$.

2.1. 2D acoustic equations

Let the non-dimensionalized pressure and velocity $\mathbf{u} = [p, u, v]^T$ satisfy the system of linearized isothermal Euler equations:

$$\begin{aligned} \partial_t p + a_o(\tilde{Q}p + \partial_x u + \partial_y v) &= 0 \\ \partial_t u + a_o(\tilde{Q}u + \partial_x p) &= 0 \\ \partial_t v + a_o(\tilde{Q}v + \partial_y p) &= 0 \end{aligned} \tag{2.1}$$

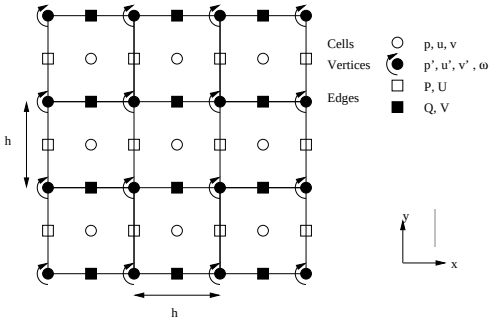

Figure 1. Grid representation

where $\tilde{Q} = [M_x\partial_x + M_y\partial_y]$ is the advection operator with constant advection $\vec{M} = (M_x, M_y)$. For the pure acoustic case $M_x = M_y = 0$. Taking the curl of the acoustic equations will give $\partial\tilde{\omega}/\partial t = 0$ implying that vorticity is time independent. A vorticity preserving scheme for the pure acoustics must satisfy $\partial\tilde{\omega}/\partial t = 0$, at least at the discrete level.

As discussed in [11], vorticity preservation depends on the choice of discretization. The discretization is chosen such that the main variables are conserved within the cell and vorticity is preserved (Fig. 1) at the vertices since this configuration produces the least odd-even decoupling mode. Note that cell coordinates are denoted by (i, j) whereas vertex coordinates are given by $(i \pm 1/2, j \pm 1/2)$. The notations developed by [11] will also be adopted, particularly the discrete average (μ) and differential (δ) operators, but new notations will also be introduced. The precise definition of these discrete operators and their properties are included in appendix A. To achieve discrete conservation, the acoustic equations are discretized as a cell-centered finite volume method

$$(\mathbf{u}^{n+1} - \mathbf{u}^n)h^2 + (\delta_x\mathbf{f}^* + \delta_y\mathbf{g}^*)h\Delta t = 0 \tag{2.2}$$

where $(\mathbf{f}^*, \mathbf{g}^*)$ are the numerical fluxes in (x, y) directions to be determined under a certain constraint in order to preserve vorticity. Let $\nu = a_o\Delta t/h$, hence

$$\mathbf{u}^{n+1} - \mathbf{u}^n = -\nu[(\delta_x U + \delta_y V), \delta_x P, \delta_y Q]^T \tag{2.3}$$

Usually a central difference is used to discretize vorticity but to minimize the spurious modes, the compact vorticity is preferred, which is defined as

$$\omega = \mu_y\delta_x v - \mu_x\delta_y u = L_\omega(\mathbf{u}) \tag{2.4}$$

implying that vertex vorticity will depend on four surrounding cell-centered velocities that encapsulate the vertex. Preserving compact vorticity requires

$$\begin{aligned} 0 = \omega^{n+1} - \omega^n &= L_\omega(\mathbf{u}^{n+1} - \mathbf{u}^n) \\ &= -\nu[0, -\mu_x\delta_y, \mu_y\delta_x][(\delta_x U + \delta_y V), \delta_x P, \delta_y Q]^T \\ &= -\nu\delta_x\delta_y(\mu_x P - \mu_y Q) \end{aligned} \tag{2.5}$$

which implies that

$$\mu_x P = \mu_y Q \tag{2.6}$$

Since the main variables are cell-centered formulations, the edge values (P,Q) must come from (p,u,v) and there exists a vertex pressure $r^{'}$ satisfying $P=\mu_y r'$, $Q=\mu_x r'$ which complies with Equation (2.6). To obtain a second order accuracy on a 9-point stencil via Taylor series expansion for p requires that

$$r' = \mu_x\mu_y p - \frac{\nu}{2}(\mu_y\delta_x u + \mu_x\delta_y v) + O(\Delta t^2, h^2) \tag{2.7}$$

Overall, the updated discrete velocities that preserve vorticity are given by

$$u^{n+1} = u^n - \nu\mu_y\delta_x r' \tag{2.8}$$

$$v^{n+1} = v^n - \nu\mu_x\delta_y r' \tag{2.9}$$

A similar discretization is done to determine the discrete second order update of pressure via edge velocities (U,V) and the details are available in [11].

Let I be the identity matrix and A_δ is a discrete spatial-operator for the acoustic equations denoted by

$$A_\delta = \begin{bmatrix} 0 & \mu_y\delta_x & \mu_x\delta_y \\ \mu_y\delta_x & 0 & 0 \\ \mu_x\delta_y & 0 & 0 \end{bmatrix} \tag{2.10}$$

thus the evolution of $\mathbf{u}$ can be written as as a two-step scheme with

$$\mathbf{u}^{'} = \left[\mu_x\mu_y I - \frac{\nu}{2}A_\delta\right]\mathbf{u}^n \tag{2.11}$$

to provide intermediate solution at the vertices. The full step

$$\mathbf{u}^{n+1} = \mathbf{u}^n - \nu A_\delta \mathbf{u}^{'} \tag{2.12}$$

uses half-step solutions to update the cells. This is the Rotated Richtmyer (RR) scheme [11] which is inherently multidimensional and has properties of second order accuracy with conservation, symmetry of operators and most importantly vorticity preserving. Note that for the acoustic equations, vorticity preservation is only dependent on how the pressure terms at the edges of the cells in the velocity equations are evaluated (Equation (2.6)).

2.2. Vorticity analysis with limiters in 2D acoustic equations

The limiting procedure at the half-step is based on one-dimensional considerations [18, 20]. It could be argued that using a one dimensional-type limiter is in conflict with the essence of vorticity which is inherently multi-dimensional. However, to the author's knowledge, nobody has rigorously investigated the concept of one dimensional limiting when preserving vorticity using the constrained-transport philosophy. Consider the following.

Lemma 2.1. *For any discrete pressure $r^{'} = f(x,y,t)$ defined at a vertex with f being an arbitrary function, the Rotated Richtmyer scheme preserves vorticity at the vertices when solving the two-dimensional acoustic equations.*

Proof. Let (P,Q) to be pressures located at the vertical and horizontal interfaces. Assume $f(x,y,t)$ to be any function defined at the vertices such that

$$\begin{aligned} P &= \mu_y r^{'} = \mu_y f(x,y,t) \\ Q &= \mu_x r^{'} = \mu_x f(x,y,t) \end{aligned} \tag{2.13}$$

The commutative property of the discrete averaging operators implies that $\mu_x\mu_y f(x,y,t) = \mu_y\mu_x f(x,y,t)$ which is equivalent to Equation (2.6) ∎

Corollary 2.1. *The Rotated Richtmyer scheme is vorticity preserving when solving the two-dimensional acoustic equations if a one-dimensional type of limiter is used for all variables provided that the pressure at the cell edges originate from the vertices.*

Using this knowledge, a limiting procedure for the RR scheme will be developed. The slope of the vertex variables can be computed via compact differencing using four cell values surrounding the vertex. Define Δ_x the discrete slope at the vertices in the x-direction

$$\Delta_x \mathbf{u}^{'} = \mu_y \delta_x \mathbf{u} \tag{2.14}$$

Referring to Fig 2, in order to limit the slopes of any variable at vertex M, three adjacent slopes are required $\Delta_x \mathbf{u}_L^{'}, \Delta_x \mathbf{u}_M^{'}, \Delta_x \mathbf{u}_R^{'}$ with slope ratios

$$\mathbf{r}_L = \frac{\Delta_x \mathbf{u}_M^{'}}{\Delta_x \mathbf{u}_L^{'}} \tag{2.15}$$

$$\mathbf{r}_R = \frac{\Delta_x \mathbf{u}_M^{'}}{\Delta_x \mathbf{u}_R^{'}} \tag{2.16}$$

The limiting step for the pressure and velocity slopes are

$$\phi_{x,M}^{p} = \min\left[\max\left(0.0, \min\left(r_L^{p}, 1.0\right)\right), \max\left(0.0, \min\left(r_R^{p}, 1.0\right)\right)\right] \tag{2.17}$$

$$\phi_{x,M}^{u,v} = \min\left[\max\left(0.0, \min\left(r_L^{u,v}, 1.0\right)\right), \max\left(0.0, \min\left(r_R^{u,v}, 1.0\right)\right)\right] \tag{2.18}$$

which will give the limited coefficients $(\phi_x^p, \phi_x^u, \phi_x^v)$ in the x-direction based on a minmod limiter [18]. Other limiters can also be used and a similar procedure is done in the y-direction. Let

$$\mathbf{q}_x = \left[\phi_x^p, \phi_x^u, \phi_x^v\right]^T \tag{2.19}$$

$$\mathbf{q}_y = \left[\phi_y^p, \phi_y^u, \phi_y^v\right]^T \tag{2.20}$$

The limited compact differencings can be written as

$$\mu_y \delta_x^{lim} \mathbf{u} = \left[\mathbf{q}_x\left(\nu^2 - \nu\right) + \nu\right] \mu_y \delta_x \mathbf{u} \tag{2.21}$$

$$\mu_x \delta_y^{lim} \mathbf{u} = \left[\mathbf{q}_y\left(\nu^2 - \nu\right) + \nu\right] \mu_x \delta_y \mathbf{u} \tag{2.22}$$

where a choice $\mathbf{q}_{x,y} = [1,1,1]^T$ will give the RR scheme whereas $\mathbf{q}_{x,y} = [0,0,0]^T$ will result in a first order scheme. Essentially, the limiting procedure is merely varying the coefficients (specificially the Courant numbers) that multiply the fluxes to produce first order or second order accurate (RR) scheme or anything in between. The variation of Courant numbers will be used later in the analysis of demonstrating the how limiting will affect vorticity preservation. The limited half-step operator is given

$$A_\delta^{lim} = \begin{bmatrix} 0 & \mu_y \delta_x^{lim} & \mu_x \delta_y^{lim} \\ \mu_y \delta_x^{lim} & 0 & 0 \\ \mu_x \delta_y^{lim} & 0 & 0 \end{bmatrix} \tag{2.23}$$

The limited half-step of the RR scheme is written as

$$\mathbf{u}^{'} = \left[\mu_x\mu_y I - \frac{1}{2\nu} A_\delta^{lim}\right] \mathbf{u}^n \tag{2.24}$$

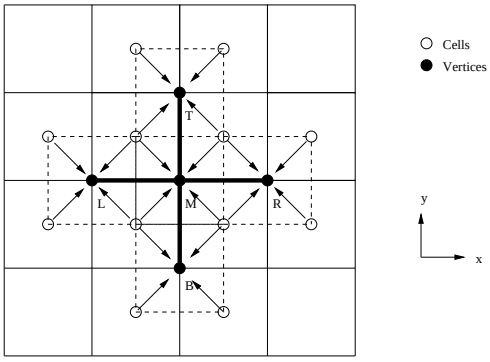

Figure 2. Limiting procedure. First, compute the slopes at the vertices via compact differencing using values at four surrounding cells (line with arrows). Then perform limiting on these slopes based on adjacent vertices (L,R) and (B,T) to the middle vertex M dimension by dimension (thick solid lines) before performing half step.

whereas the full step is the same as before (Equation (2.12)).

3. Vorticity analysis in 2D linearized Euler

The curl of the linearized Euler equations (Equation 2.2) provides the analytical inviscid vorticity transport equation $\partial\tilde{\omega}/\partial t + \tilde{Q}\tilde{\omega} = 0$. Discretely, this means

$$\mathbf{u}^{n+1} - \mathbf{u}^n = -\nu T_\delta \left[\mu_x\mu_y I - \frac{1}{2}\nu T_\delta\right]\mathbf{u}^n = -\nu T_\delta \mathbf{u}^{'} \tag{3.1}$$

where

$$T_\delta = \begin{bmatrix} \tilde{Q}_\delta & \mu_y\delta_x & \mu_x\delta_y \\ \mu_y\delta_x & \tilde{Q}_\delta & 0 \\ \mu_x\delta_y & 0 & \tilde{Q}_\delta \end{bmatrix} = \tilde{Q}_\delta I + A_\delta \tag{3.2}$$

and that the discrete advection operator is

$$\tilde{Q}_\delta = [M_x\mu_y\delta_x + M_y\mu_x\delta_y] \tag{3.3}$$

The change of discrete vorticity is

$$\begin{aligned} \omega^{n+1} - \omega^n &= L_\omega[\mathbf{u}^{n+1} - \mathbf{u}^n] = -\nu L_\omega T_\delta \mathbf{u}^{'} \\ &= -\nu L_\omega(\tilde{Q}_\delta I + A_\delta)\mathbf{u}^{'} = -\nu\tilde{Q}_\delta L_\omega \mathbf{u}^{'} = -\nu\tilde{Q}_\delta\omega^{'} \end{aligned} \tag{3.4}$$

provided that condition (2.6) is satisfied which overall implies consistency between the vorticity predicted by the vorticity transport equation and vorticity deduced from the discrete velocities, where

$$\omega^{'} = \mu_y\delta_x v' - \mu_x\delta_y u' \tag{3.5}$$

is the *cell vorticity based on vertex velocities*. This further implies that the numerical vorticity evolution depends on the half-step velocities which creates some restrictions when limiting these velocities.

3.1. Vorticity analysis with limiters

As discussed in Section 2.2, flux limiting can be done by varying the Courant numbers that are multiplied to each component of the flux-gradients. Again, the limiting procedure is based on one dimensional considerations, and for simplicity the analysis will be on irrotational flow. Irrotationality implies that the numerical vorticity evolution is zero for all times ($\omega^n = 0$) which in turn requires that the cell-vorticity to be also zero ($\omega^{'} = 0$) as given by Equation (3.4). If the half step of RR scheme does not preserve vorticity, the overall scheme will not be vorticity preserving. This imposes a restriction for the half-step velocities located at the vertices, which are computed from cell quantities (Equation (2.11))

$$u' = \mu_x\mu_y u - \frac{\nu_U}{2}\tilde{Q}_\delta u - \frac{\nu_P}{2}\mu_y\delta_x p \tag{3.6}$$

$$v' = \mu_x\mu_y v - \frac{\nu_U}{2}\tilde{Q}_\delta v - \frac{\nu_P}{2}\mu_x\delta_y p \tag{3.7}$$

where the Courant numbers with respect to velocity ν_U and pressure ν_P components are introduced. Inserting the previous equations into Equation (3.5)

$$\begin{aligned}\omega^{'} = \mu_x\mu_y(\mu_y\delta_x v - \mu_x\delta_y u) - \frac{1}{2}[\mu_y\delta_x(\nu_U\tilde{Q}_\delta v) - \mu_x\delta_y(\nu_U\tilde{Q}_\delta u)\\ + \mu_y\delta_x(\nu_P\mu_x\delta_y p) - \mu_x\delta_y(\nu_P\mu_y\delta_x p)]\end{aligned} \tag{3.8}$$

The first line of this equation is the initial vorticity and is zero for discretely irrotational flow. The second line is the discrete advection component which may cause spurious vorticity ($\omega_U^{'}$). However this second term also contains the physical vorticity which will be shown later. The last line corresponds to spurious vorticity due to pressure gradients denoted by $\omega_P^{'}$.

Assume that each component that may produce spurious vorticity is treated independently and that the Courant numbers (ν_U, ν_P) are local variables located at the vertices to accommodate the process of limiting.

Theorem 3.1. *For the RR scheme, if $\mu_y\delta_x v = \mu_x\delta_y u$ at each vertex, $\omega_{=}^{'}0 \Leftrightarrow \nu_P = k_1$ and $\nu_U = k_2$ at each vertex where k_1 and k_2 are constants.*

The proof of this theorem is rather lengthy and is provided in Appendix B. The implication of this theorem is that a local flux-limiting which is necessary to circumvent Godunov's Theorem will destroy the vorticity preserving property of the RR scheme when solving the linearized Euler equations.

Before the numerical results are presented, define

$$T_\delta^{lim} = \begin{bmatrix} M_x\mu_y\delta_x^{lim} + M_y\mu_x\delta_y^{lim} & \mu_y\delta_x^{lim} & \mu_x\delta_y^{lim} \\ \mu_y\delta_x^{lim} & M_x\mu_y\delta_x^{lim} + M_y\mu_x\delta_y^{lim} & 0 \\ \mu_x\delta_y^{lim} & 0 & M_x\mu_y\delta_x^{lim} + M_y\mu_x\delta_y^{lim} \end{bmatrix} \tag{3.9}$$

to be a limited version of Equation (3.2) where $\mu_y\delta_x^{lim}$ and $\mu_y\delta_x^{lim}$ are the limited compact differencing as presented in Section 2.2. Then the limited half-step RR scheme will be

$$\mathbf{u}^{'} = \left[\mu_x\mu_y I - \frac{1}{2\nu}T_\delta^{lim}\right]\mathbf{u}^n \tag{3.10}$$

providing temporal solution at the vertices.

The full step of the limited RR scheme solving the linearized Euler would be

$$\mathbf{u}^{n+1} = \mathbf{u}^n - \nu[\delta_x \mathbf{f}^* + \delta_y \mathbf{g}^*] \tag{3.11}$$

where the numerical fluxes depend on the half-step variables ($\mathbf{u}^{'}$) obtained from Equation (3.10) given by

$$\mathbf{f}^* = \begin{bmatrix} M_x \mu_y p^{'} + \mu_y u^{'} \\ M_x \mu_y u^{'} + \mu_y p^{'} \\ M_x \mu_y v^{'} \end{bmatrix} \tag{3.12}$$

$$\mathbf{g}^* = \begin{bmatrix} M_y \mu_x p^{'} + \mu_x u^{'} \\ M_y \mu_x u^{'} \\ M_y \mu_x v^{'} + \mu_x p^{'} \end{bmatrix} \tag{3.13}$$

4. Numerical results

In the two dimensional inviscid approach of preserving vorticity, there are two main elements that must be controlled. The first is the acoustics which is due to the pressure of the fluid. The second, is the advection term which represents the transport of vorticity. Improper discretization of the pressure term or the advection terms will generate spurious vorticities in the computation as discussed in the previous sections. There are also discussions in the literature in which acoustics effect are dominant in certain SVI problems [5] thus it is important to look at the acoustics at the simplest set up.

The test cases utilized in this paper are aimed to evaluate the effects of vortical computations based on purely acoustics and acoustics combined with constant advection. The latter is also known as the linearized Euler equations. Since this is a proof-of-concept paper, the test cases herein are designed to be as simple as possible for the purpose of verifying the theoretical results in this study. One of the test cases also has exact solutions that can be used for precise comparisons with numerical data.

4.1. Irrotational flows for 2D acoustics

The following problem with an exact solution will be used as test Case 1:

$$\begin{aligned} p &= -\sqrt{2}\sin kx \sin ky \cos\sqrt{2}kt \\ u &= \cos kx \sin ky \sin\sqrt{2}kt \\ v &= \sin kx \cos ky \sin\sqrt{2}kt \end{aligned} \tag{4.1}$$

The equations above satisfy Equation (2.1) for $M_x = M_y = 0$ using hard boundary (solid wall) conditions with $k = \pi/2$. The computational domain D $\in$ [-1,1] x [-1,1] uses 40 x 40 cells with $\nu = 0.5$. The numerical results are compared with the exact solution at $t = 0.25$. Numerical results for three schemes are included: the RR scheme, RR scheme with centered vorticity discretization (RR-c), and the RR scheme with minmod limiter (RR-M). The results are shown in Figure 3.

For conciseness, only the U-velocity error contours are included. The V-velocity and pressure error results are similar hence omitted. Overall, both the RR and RR-M produce errors which are less than 3 percent compared to the exact solution. However, the RR-M error contours are not smooth due to the effects of nonlinearity from the minmod limiter.

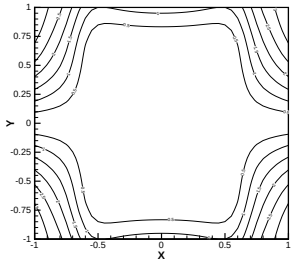

Figure 3. (a)U velocity error for RR (test 1).

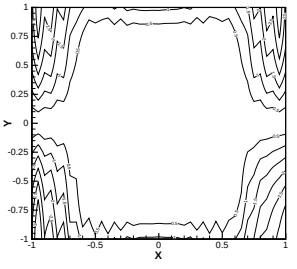

Figure 3. (b)U velocity error for RR-M (test 1).

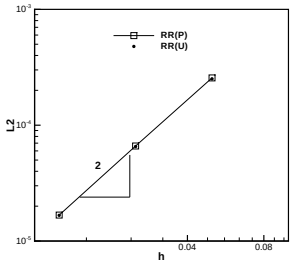

Figure 4. L_2 norms for RR (test 1).

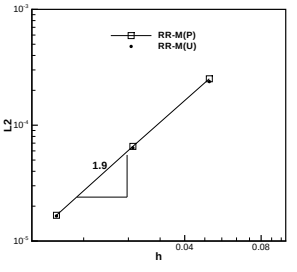

Figure 5. L_2 norms for RR-M.

In addition, the grid study results indicate that only the RR scheme is purely second order accurate in space (Fig. 4) whereas the RR-M scheme is slightly less than second order (Fig. 5). This small difference in order of accuracy is due to the minmod limiter slightly reducing the order of accuracy of the RR-M scheme, which is to be expected for a relatively smooth data.

Most importantly, both schemes exactly preserve irrotationality of the flow. This confirms that one dimensional type limiters will not destroy the vorticity preserving qualities of the Rotated-Rictmyer scheme, at least for the acoustic equations. Note that the RR scheme will not be vorticity preserving if vorticity is discretely computed using other than the compact vorticity, consistent with the theory [11]. The spurious vorticity at $t = 0.25$ is in $O(10^{-2})$ and will increase in magnitude with time.

4.2. Rotational flow for 2D acoustics

The following initial value problem will be used as test Case 2:

$$
\begin{aligned}
p &= 1.0 - 0.25\frac{c_1^2}{c_2}\left(\exp\left[-2c_2\left([x-x_p]^2+[y-y_p]^2\right)\right]-1\right)\\
u &= c_1[y-y_v]\exp\left[-c_2\left([x-x_v]^2+[y-y_v]^2\right)\right]\\
v &= -c_1[x-x_v]\exp\left[-c_2\left([x-x_v]^2+[y-y_v]^2\right)\right]
\end{aligned}
\tag{4.2}
$$

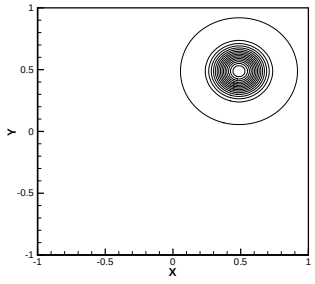

Figure 6. (a) ω via RR and RR-M scheme for $t \geq 0$(test 2).

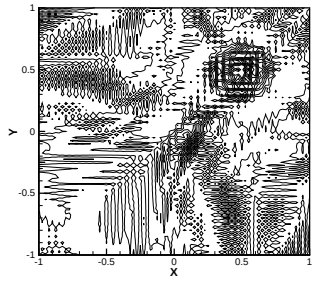

Figure 6. (b) ω via CC scheme at t=2.5.

with perturbation coefficients $c_1 = c_2 = 20.0$. The vortex center is located at $(x_v, y_v) = (0.5, 0.5)$ while the pressure center is located at $(x_p, y_p) = (0,0)$. The computational domain D $\in$ [-1,1] x [-1,1] uses 80 x 80 cells with $\nu = 0.5$ and periodic boundary conditions are enforced. This problem demonstrates an unsteady acoustic interaction with a vortex but the vortex should remain unchanged for all times. The results are shown in Fig. 6.

The pressure and velocity results are visibly similar between the RR, RR-M and the conventional central (CC) schemes hence not included. The striking thing is that the predicted vorticity results of the CC are vastly different from the vorticity predicted by the RR and RR-M scheme. The initial pressure wave captured via CC scheme creates spurious vortices that will undergo a complex interaction with the physical vortex. As a result, the physical vortex cannot be preserved. The generation of spurious vorticity has been previously reported [2] and the results here reconfirm the existence of unphysical vorticity. Despite the complex wave interactions, the physical vortex is preserved for all times when computed by the RR and RR-M schemes as shown in Fig. 6. Note that the ω predicted by the RR and RR-M scheme is the exact ω for $t \geq 0$ confirming that vorticity is preserved.

4.3. Irrotational flows for 2D linearized Euler

Define a two dimensional computational domain, $D \in [-2,2] \times [-2,2]$ using 80×80 cells with the following initial value problem (test Case 3).

$$p = 1.0 - 0.25\frac{c_1^2}{c_2}\big(\exp\big[-2c_2\big([x-x_o]^2 + [y-y_o]^2\big)\big] - 1\big)$$

$$(u,v) = (0,0) \tag{4.3}$$

where $(c_1, c_2) = (\pi/2, \pi/2)$. The reference coordinates are chosen to be $(x_o, y_o) = (-1,-1)$ and a uniform constant advection with $(M_x, M_y) = (1.0, 1.0)$ is prescribed. Periodic boundary conditions are used and a Courant number $\nu = 0.25$ with $a_0 = 1.0$ are chosen. The goal is to predict time-accurate solutions at $t = 1$. This problem will depict linear interactions between the acoustic wave (due to pressure) and velocity but nevertheless, the solution should remain irrotational.

The numerical results for pressure and velocities between the selected schemes are visibly similar as shown in Fig. 7(a)– Fig. 7(d). However, the predicted vorticity results are

vastly different (Fig. 7(e)). Although the RR scheme preserves irrotationality but the RR-M scheme produces spurious vorticity in the range of $-0.2 \leq \omega \leq 0.2$ at $t = 1$. This is consistent with the theoretical results in section 3.1 where any limiting applied to the RR scheme will compromise the vorticity preserving nature of the scheme. Table 1 shows that the spurious vorticity grows with time for the RR-M scheme.

Table 1. L_∞ norms for ω of the two schemes (test Case 3).

SCHEME	RR	RR-M
$t = 0.05$	0.0	2.2657e-4
$t = 1$	0.0	8.9687e-1

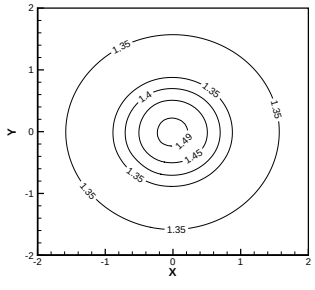

Figure 7. (a) RR pressure (test 3).

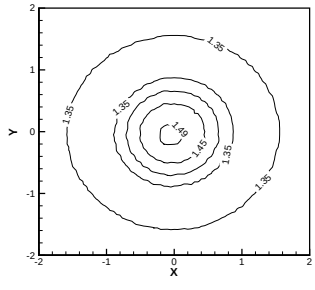

Figure 7. (b) RR-M pressure (test 3).

5. Conclusion and Future Work

In this paper, a preliminary investigation of discrete vorticity control using the limited second order Rotated Richtmyer scheme is performed. Excluding the acoustic equations, it has been shown that coupling the classical TVD limiter with Rotated Richtmyer scheme will not preserve vorticity. This is unsurprising since the RR scheme is designed using a specific local and linear averaging to preserve vorticity. Any form of nonlinearity will cause the RR scheme (strictly) to no longer be vorticity preserving. Perhaps the concept of strictly preserving vorticity (i.e. vorticity is exactly preserved) is too demanding. 'Weakly' preserving vorticity where the vorticity errors due to discretization are small is perhaps more realistic to be achieved as done by [8, 10]. However, there is a need to precisely define 'weak' vorticity preserving formulation which will be part of future work.

It must be emphasized that this work is just a preliminary study and is a long way from addressing the shock-vortex interaction problem, although it is with great hope that this study will pave the way for further investigations on limited vorticity preserving schemes.

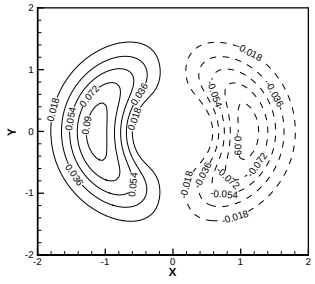

Figure 7. (c) RR U-velocity (test 3).

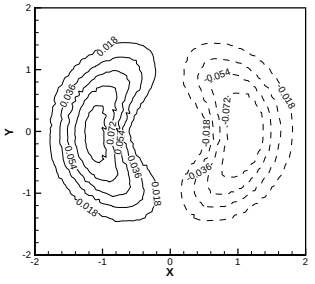

Figure 7. (d) RR-M U-velocity (test 3).

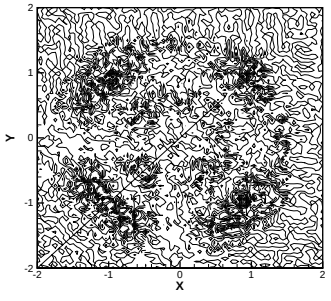

Figure 7. (e) Spurious vorticity $O(0.1)$ for RR-M (test 3).

Appendix A. Discrete Operators

Finite difference formulations will be introduced on two dimensional uniform grids based on notations of [11]. The discrete differencing and averaging operators are defined by

$$\delta_x()_{.,.} = ()_{.+\frac{1}{2},.} - ()_{.-\frac{1}{2},.} \tag{A.1}$$

$$\delta_y()_{.,.} = ()_{.,.+\frac{1}{2}} - ()_{.,.-\frac{1}{2}} \tag{A.2}$$

$$\mu_x()_{.,.} = \frac{1}{2}\left[()_{.+\frac{1}{2},.} + ()_{.-\frac{1}{2},.}\right] \tag{A.3}$$

$$\mu_y()_{.,.} = \frac{1}{2}\left[()_{.,.+\frac{1}{2}} - ()_{.,.-\frac{1}{2}}\right] \tag{A.4}$$

The result of any above operator will lie half-way between the two inputs. The product of two operators will also be used. For example, $\mu_x\delta_x()_{i,j}$ is a *central difference* of $1/2[()_{i+1,j} - ()_{i-1,j}]$ in the x-direction located at grid point i, j. Another example is the *compact difference* $\mu_y\delta_x()_{i,j}$, which involves four points $(i \pm 1/2, j \pm 1/2)$ of a square centered at grid i, j (Fig. 8). Assume prime and non-prime variables to be quantities located at the vertices and cell-center respectively. Cells are points with all integer coordinates while vertices are points with all half integer coordinates. On the other hand, points with one integer and one half integer coordinate define an edge (Fig. 1). The following operators will

be used herein.

$$\mu_x\mu_y(u) = \frac{1}{4}[(u)_{i+1,j+1} + (u)_{i,j+1} + (u)_{i,j} + (u)_{i+1,j}] \tag{A.5}$$

$$\mu_y\delta_x(u) = \frac{1}{2}[(u)_{i+1,j+1} + (u)_{i+1,j} - (u)_{i,j+1} - (u)_{i,j}] \tag{A.6}$$

$$\mu_x\delta_y(u) = \frac{1}{2}[(u)_{i+1,j+1} + (u)_{i,j+1} - (u)_{i+1,j} - (u)_{i,j}] \tag{A.7}$$

where the product of the above operators lie on a vertex with coordinates $(i+1/2, j+1/2)$. Likewise, applying these operators on the vertex quantities gives

$$\mu_x\mu_y(u') = \frac{1}{4}\left[(u')_{i+\frac{1}{2},j+\frac{1}{2}} + (u')_{i-\frac{1}{2},j+\frac{1}{2}} + (u')_{i-\frac{1}{2},j-\frac{1}{2}} - (u')_{i+\frac{1}{2},j-\frac{1}{2}}\right] \tag{A.8}$$

$$\mu_y\delta_x(u') = \frac{1}{2}\left[(u')_{i+\frac{1}{2},j+\frac{1}{2}} + (u')_{i+\frac{1}{2},j-\frac{1}{2}} - (u')_{i-\frac{1}{2},j+\frac{1}{2}} - (u')_{i-\frac{1}{2},j-\frac{1}{2}}\right] \tag{A.9}$$

$$\mu_x\delta_y(u') = \frac{1}{2}\left[(u')_{i+\frac{1}{2},j+\frac{1}{2}} + (u')_{i-\frac{1}{2},j+\frac{1}{2}} - (u')_{i+\frac{1}{2},j-\frac{1}{2},k-\frac{1}{2}} - (u')_{i-\frac{1}{2},j-\frac{1}{2},k-\frac{1}{2}}\right] \tag{A.10}$$

where the products lie on a cell with coordinates (i, j). The centered vorticity $\omega_c = \mu_x\delta_x(v) - \mu_y\delta_y(u)$ uses cell variables as input and the resulting discrete vorticity also lies on the cells. The compact vorticity defined as $\omega = \mu_y\delta_x(v) - \mu_x\delta_y(u)$, where cell variables are utilized to compute discrete vertex vorticities. The following represent product rules for the operators.

$$\mu_x(ab) = \mu_x(a)\mu_x(b) + \frac{1}{4}\delta_x(a)\delta_x(b) \tag{A.11}$$

$$\mu_y(ab) = \mu_y(a)\mu_y(b) + \frac{1}{4}\delta_y(a)\delta_y(b) \tag{A.12}$$

$$\delta_x(ab) = \mu_x(a)\delta_x(b) + \mu_x(b)\delta_x(a) \tag{A.13}$$

$$\delta_y(ab) = \mu_y(a)\delta_y(b) + \mu_y(b)\delta_y(a) \tag{A.14}$$

and the identities

$$\delta_x^2 = 4\left(\mu_x^2 - 1\right), \quad \delta_y^2 = 4\left(\mu_y^2 - 1\right) \tag{A.15}$$

which can be proven by direct computation.

Appendix B. Proof of Theorem 3.1

To prove this theorem, two lemmas will be required. Using the product rules for the operators (Equation (A.11)), the contributions from pressure gradients to spurious vorticity (last line of Equation 3.8) is

$$\begin{aligned}\omega_P^{'} &= \mu_y\delta_x(\nu_P\mu_x\delta_y p) - \mu_x\delta_y(\nu_P\mu_y\delta_x p)\\ &= \mu_y[\mu_x\nu_P\delta_x(\mu_x\delta_y p) + \mu_x(\mu_x\delta_y p)\delta_x\nu_P] - \mu_x[\mu_y\nu_P\delta_y(\mu_y\delta_x p) + \mu_y(\mu_y\delta_x p)\delta_y\nu_P]\end{aligned}$$

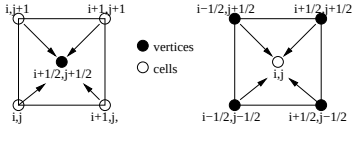

Figure 8. Product of two operators on cells and vertices

$$
\begin{aligned}
&= (\mu_y\mu_x\nu_P)(\mu_x\mu_y\delta_x\delta_y p) + \frac{1}{4}(\mu_x\delta_y\nu_P)(\mu_x\delta_x\delta_y^2 p) + (\mu_x^2\mu_y\delta_y p)(\mu_y\delta_x\nu_P) \\
&\quad + \frac{1}{4}(\mu_x^2\delta_y^2 p)(\delta_x\delta_y\nu_P) - (\mu_y\mu_x\nu_P)(\mu_x\mu_y\delta_x\delta_y p) - \frac{1}{4}(\mu_y\delta_x\nu_P)(\mu_y\delta_x^2\delta_y p) \\
&\quad - (\mu_x\mu_y^2\delta_x p)(\mu_x\delta_y\nu_P) - \frac{1}{4}(\mu_y^2\delta_x^2 p)(\delta_x\delta_y\nu_P) \\
&= \frac{1}{4}(\delta_x\delta_y\nu_P)(\mu_x^2\delta_y^2 - \mu_y^2\delta_x^2)p + (\mu_y\delta_x\nu_P)(\mu_x^2\mu_y\delta_y - \frac{1}{4}\mu_y\delta_x^2\delta_y)p \\
&\quad - (\mu_x\delta_y\nu_P)(\mu_x\mu_y^2\delta_x - \frac{1}{4}\mu_x\delta_x\delta_y^2)p \qquad \text{(B.1)}
\end{aligned}
$$

Using identities available (Equation (A.15)), the previous equation is reduced to

$$
\begin{aligned}
\omega_P^{'} &= (\delta_x\delta_y\nu_P)[\mu_x^2(\mu_y^2-1) - \mu_y^2(\mu_x^2-1)]p + (\mu_y\delta_x\nu_P)[\mu_x^2\mu_y\delta_y - (\mu_x^2-1)(\mu_y\delta_y)]p \\
&\quad - (\mu_x\delta_y\nu_P)[\mu_x\mu_y^2\delta_x - (\mu_y^2-1)(\mu_x\delta_x)]p \\
&= \delta_x\delta_y\nu_P[\mu_y^2 - \mu_x^2]p + \mu_y\delta_x\nu_P(\mu_y\delta_y)p - \mu_x\delta_y\nu_P(\mu_x\delta_x)p \\
&= \delta_y(\mu_y p\delta_x\nu_P) - \delta_x(\mu_x p\delta_y\nu_P) \qquad \text{(B.2)}
\end{aligned}
$$

Lemma B.1. *$\omega_P^{'} = 0 \Leftrightarrow \nu_P = k$ at each vertex, where k is a constant.*

Proof. Assume $\omega_P^{'} = 0$ with different ν_P at each vertex and define $p = xy$ at each cell in $D \in$ [2,4] x [2,4]. But in D_s which is a subset of D (Fig. 9),

$$
\begin{aligned}
\omega_P^{'} &= (p_O + p_N)(\nu_1 - \nu_2) - (p_O + p_S)(\nu_4 - \nu_3) \\
&\quad - (p_O + p_E)(\nu_1 - \nu_4) + (p_O + p_W)(\nu_2 - \nu_3) \\
&= (\nu_4 - \nu_1)p_E + (\nu_1 - \nu_2)p_N + (\nu_2 - \nu_3)p_W + (\nu_3 - \nu_4)p_S \\
&= (\nu_4 - \nu_1)x_E y_E + (\nu_1 - \nu_2)x_N y_N + (\nu_2 - \nu_3)x_W y_W + (\nu_3 - \nu_4)x_S y_S \\
&= 0
\end{aligned}
$$

only if $\nu_1 = \nu_2 = \nu_3 = \nu_4$ (contradiction). Now if ν_P is identical on each vertex, it is obvious that $\omega_P^{'} = 0$ at the vertices which completes the proof. ∎

Corollary B.1. *It is a necessary condition to have ν_P identical at each vertex for the Rotated Richtmyer scheme to be vorticity preserving when solving the linearized Euler equations.*

Now the effects of advection in generating spurious vorticity (second line of Equation (3.8)) will be investigated.

$$
\begin{aligned}
\omega_U^{'} &= \mu_y\delta_x(\nu_U\tilde{Q}_\delta v) - \mu_x\delta_y(\nu_U\tilde{Q}_\delta u) \\
&= \mu_y[(\mu_x\nu_U)(\delta_x\tilde{Q}_\delta v) + (\mu_x\tilde{Q}_\delta v)(\delta_x\nu_U)] - \mu_x[(\mu_y\nu_U)(\delta_y\tilde{Q}_\delta u) + (\mu_y\tilde{Q}_\delta u)(\delta_y\nu_U)] \\
&= (\mu_x\mu_y\nu_U)\tilde{Q}_\delta(\mu_y\delta_x v - \mu_x\delta_y u) + \frac{1}{4}(\delta_x\delta_y\nu_U)\tilde{Q}_\delta(\mu_x\delta_y v - \mu_y\delta_x u) \\
&\quad + (\mu_y\delta_x\nu_U)\tilde{Q}_\delta(\mu_x\mu_y v - \frac{1}{4}\delta_x\delta_y u) - (\mu_x\delta_y\nu_U)\tilde{Q}_\delta(\mu_x\mu_y u - \frac{1}{4}\delta_x\delta_y v) \qquad \text{(B.3)}
\end{aligned}
$$

The first term of the previous equation represents discrete vorticity being transported and for irrotational flow, this term is zero. However, the remaining terms are spurious vorticity

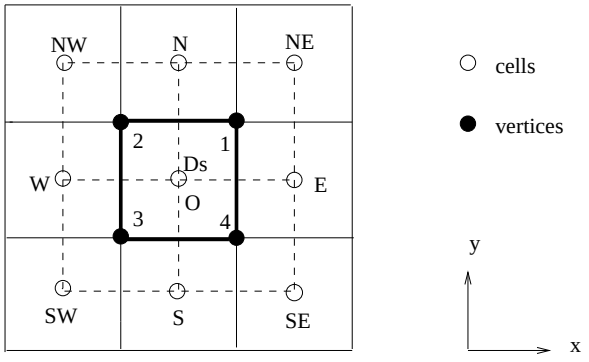

Figure 9. Subdomain D_s centered at cell O. To preserve vorticity at cell O which is bounded by vertices 1,2,3 and 4, all v must be identical at these vertices.

being transported hence $\omega_U^{'}$ reduces to

$$\omega_U^{'} = (\mu_x\delta_y v_U)\tilde{Q}_\delta(\mu_x\mu_y v - \frac{1}{4}\delta_x\delta_y u) - (\mu_y\delta_x v_U)\tilde{Q}_\delta(\mu_x\mu_y u - \frac{1}{4}\delta_x\delta_y v)$$

$$+\frac{1}{4}(\delta_x\delta_y v_U)\tilde{Q}_\delta(\mu_x\delta_y v - \mu_y\delta_x u) \tag{B.4}$$

Lemma B.2. *$\omega_U^{'} = 0 \Leftrightarrow v_U = k$ at each vertex, where k is a constant.*

Proof. Again, another proof via contradiction. Define an irrotational velocity distribution $(u,v) = (x^2,0)$ at each cell with $(M_x,M_y) = (1,0)$ and distinct v_U at each vertex in D as before (Fig. 9). However, in D_s,

$$\begin{aligned}
\omega_U^{'} &= \frac{1}{16}(v_1 - v_4 + v_2 - v_3)M_x\Big(v_{NE} + 2v_E + v_{SE} - v_{SW} - 2v_W - v_{NW} \\
&\quad - \frac{1}{4}(u_{NE} + 2u_N + u_{SW} - u_{NW} - 2u_S - u_{SE})\Big) \\
&\quad - \frac{1}{16}(v_1 - v_2 + v_4 - v_3)M_x\Big(u_{NE} + 2u_E + u_{SE} - u_{SW} - 2u_W - u_{NW} \\
&\quad - \frac{1}{4}(v_{NE} + 2v_N + v_{SW} - v_{NW} - 2v_S - v_{SE})\Big) \\
&\quad + \frac{1}{4}(v_1 - v_4 - (v_2 - v_3))M_x(v_{NW} - v_{SW} \\
&\quad - (u_{NE} - 2u_N + u_{NW} + 2u_E + 2u_W + u_{SE} - 2u_S - 4u_O + u_{SW})) \\
&= \frac{-1}{64}(v_1 - v_4 + v_2 - v_3)(x_{NE}^2 + 2x_N^2 + x_{SW}^2 - x_{NW}^2 - x_S^2 - x_{SE}^2) \\
&\quad - \frac{1}{16}(v_1 - v_2 + v_4 - v_3)(x_{NE}^2 + 2x_E^2 + x_{SE}^2 - x_{SW}^2 - 2x_W^2 - x_{NW}^2) \\
&\quad - \frac{1}{4}(v_1 - v_4 + v_3 - v_2)(x_{NE}^2 - 2x_N^2 + x_{NW}^2 + 2x_E^2 + 2x_W^2 + x_{SE}^2 - 2x_S^2 - 4x_O^2 + x_{SW}^2)
\end{aligned}$$

Obviously $\omega_U^{'} = 0 \Rightarrow v_1 = v_2 = v_3 = v_4$. If v_U is identical at each vertex it is easy to see that $\omega_U^{'} = 0$ at all vertices, completing proof of Theorem 3.1. ∎

Acknowledgement. This research was supported by Universiti Sains Malaysia short term grants 304/PAERO/ 6039014 and 304/AERO/60311026.

References

[1] D. Drikakis, L. Margolin and P. K. Smolarkiewicz, On "spurious" eddies, *Int. J. Num. Meth. Fluids* **40** (2002), 313–322.

[2] D. Drikakis and P. K. Smolarkiewicz, On spurious vortical structures, *J. Comput. Phys.* **172** (2001), no. 1, 309–325.

[3] M. Fey and M. Torrilhon, Vorticity preserving finite volume method for the wave equation system, in *Hyperbolic Problems: Theory, Numerics and Applications. I*, 129–137, Yokohama Publ., Yokohama, 2006.

[4] S. K. Godunov, A difference method for numerical calculation of discontinuous solutions of the equations of hydrodynamics, *Mat. Sb. (N.S.)* **47 (89)** (1959), 271–306.

[5] F. Graso and S. Pirozzoli, Shock wave vortex interactions: Shock and vortex deformations, and sound production, *Theoret. Comp. Fluid Dynamics* **13** (2000), 421–456.

[6] A. Harten, High resolution schemes for hyperbolic conservation laws, *J. Comput. Phys.* **49** (1983), no. 3, 357–393.

[7] F. Ismail, P. M. Carrica, T. Xing and F. Stern, Evaluation of linear and nonlinear convection schemes on multidimensional non-orthogonal grids with applications to KVLCC2 tanker, *Internat. J. Numer. Methods Fluids* **64** (2010), no. 8, 850–886.

[8] F. Ismail and P. L. Roe, Toward a vorticity preserving second order finite volume scheme solving the Euler equations, in Proceedings of 17th CFD Conference (Toronto), AIAA, Canada, 2005, pp. 2005–5235.

[9] F. Ismail and P. L. Roe, Affordable, entropy-consistent Euler flux functions. II. Entropy production at shocks, *J. Comput. Phys.* **228** (2009), no. 15, 5410–5436.

[10] A. Lerat, F. Falissard and J. Sidès, Vorticity-preserving schemes for the compressible Euler equations, *J. Comput. Phys.* **225** (2007), no. 1, 635–651.

[11] K. W. Morton and P. L. Roe, Vorticity-preserving Lax-Wendroff-type schemes for the system wave equation, *SIAM J. Sci. Comput.* **23** (2001), no. 1, 170–192 (electronic).

[12] W. Oh, J. Kim and O. Kwon, Numerical simulation of two dimensional blade vortex interactions using unstructured adaptive meshes, *AIAA Journal* **40** (2002), 474–480.

[13] S. Pirozzoli, Numerical methods for high-speed flows, in *Annual Review of Fluid Mechanics. Volume 43, 2011*, 163–194, Annu. Rev. Fluid Mech., 43 Annual Reviews, Palo Alto, CA.

[14] A. Rault, G. Chiavassa and R. Donat, Shock-vortex interactions at high Mach numbers, *J. Sci. Comput.* **19** (2003), no. 1-3, 347–371.

[15] P. L. Roe, Computational fluid dynamics—retrospective and prospective, *Int. J. Comput. Fluid Dyn.* **19** (2005), no. 8, 581–594.

[16] N. D. Sandham, Q. Li and H. C. Yee, Entropy splitting for high-order numerical simulation of compressible turbulence, *J. Comp. Physics* **178** (2002), 307–322.

[17] P. K. Subbareddy and G. V. Candler, A fully discrete, kinetic energy consistent finite-volume scheme for compressible flows, *J. Comput. Phys.* **228** (2009), no. 5, 1347–1364.

[18] P. K. Sweby, High resolution schemes using flux limiters for hyperbolic conservation laws, *SIAM J. Numer. Anal.* **21** (1984), no. 5, 995–1011.

[19] E. Tadmor, The numerical viscosity of entropy stable schemes for systems of conservation laws. I, *Math. Comp.* **49** (1987), no. 179, 91–103.

[20] B. Van Leer, Toward the ultimate conservative difference scheme V. A second order sequel to Godunov's method, *J. Comp. Physics* **32** (1979), 101–136.